Numerical methods for Riemann–Hilbert problems in multiply connected circle domains

CrossMark

R. Balu, T.K. DeLillo *

Department of Mathematics, Statistics, and Physics, Wichita State University, Wichita, KS 67260-0033, USA

ARTICLE INFO

ABSTRACT

Riemann–Hilbert problems in multiply connected domains arise in a number of applications, such as the computation of conformal maps. As an example here, we consider a linear problem for computing the conformal map from the exterior of m disks to the exterior of m linear slits with prescribed inclinations. The map can be represented as a sum of Laurent series centered at the disks and satisfying a certain boundary condition. R. Wegmann developed a method of successive conjugation for finding the Laurent coefficients. We compare this method to two methods using least squares solutions to the problem. The resulting linear system has an underlying structure of the form of the identity plus a low rank operator and can be solved efficiently by conjugate gradient-like methods.

© 2016 Elsevier B.V. All rights reserved.

1. Introduction

Linear Riemann–Hilbert (R–H) problems arise in a number of applications, such as the computation of conformal maps [1–3]. For multiply connected domains in the complex plane, maps from domains bounded by circles are useful for computations, since Laurent series can be used to represent the functions analytic in the exterior of the disks. Here we compare numerical methods for a simple R–H problem for computing the conformal map from a domain exterior to circles to a domain exterior to a number of linear slits. The methods solve for the *Laurent coefficients* and include a method of *successive conjugation* due to Wegmann [4,3] and a method based on a *least squares solution* to the boundary value problem; see, e.g., [5,6]. We formulate the least squares problem in such a way that the resulting system has singular values well-grouped around 1 with an underlying structure of the *identity plus a low-rank matrix*. Conjugate-gradient-like methods can therefore often be used efficiently. The main point of this paper is to uncover this structure in a simple example and investigate its effect on the numerics. We expect that the analysis here will be useful for a number of other similar computational problems, such as those in [7–12].

In Section 2, we introduce the conformal map from the exterior of m given disks to the exterior of m slits with given inclinations and show that it satisfies a Riemann–Hilbert boundary value problem for a function analytic in the circular domain. Section 3 reviews Wegmann's method of successive conjugation for solving this Riemann–Hilbert problem and presents our least squares method. An analysis of the linear systems shows the grouping of the eigenvalues and their effect on the convergence of the conjugate gradient method applied to the normal equations. Section 4 gives several numerical examples showing the behavior of the methods for domains of various connectivity and cases where the circles nearly touch. Section 5 discusses possible future work. Portions of the MATLAB code are given in the Appendix.

---

* Corresponding author.
E-mail addresses: raja.balu@math.wichita.edu (R. Balu), delillo@math.wichita.edu (T.K. DeLillo).
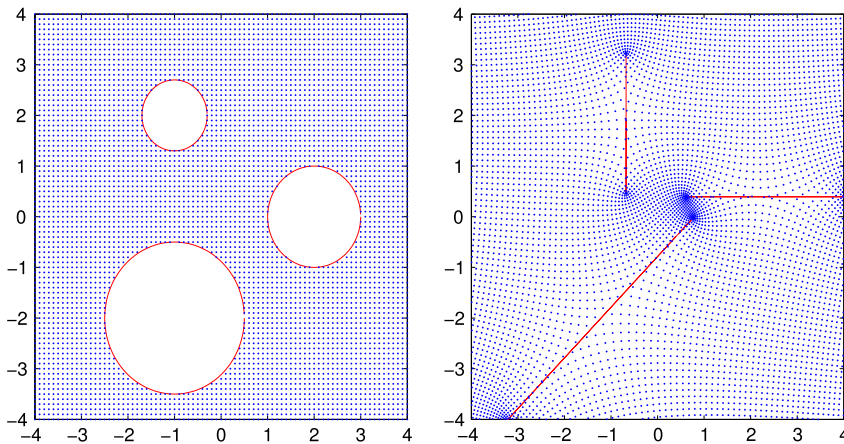
Fig. 1. Map to $m = 3$ slits from [3] with circle centers, $z_1 = 2, z_2 = -1 - 2i, z_3 = -1 + 2i$ and radii, $R_1 = 1, R_2 = 1.5, R_3 = 0.7$ and inclination angles of slits, $\alpha_1 = 0, \alpha_2 = \pi/4, \alpha_3 = \pi/2$.

2. Conformal mapping

Let G denote the domain exterior to m mutually exterior, nonoverlapping disks in the complex plane bounded by circles with centers, z_k, and radii, $R_k, \ k = 1, \ldots, m$. Since the circles do not overlap, $(R_j + R_k)/|z_j - z_k| < 1$. Wegmann [3, Eq. (390)] considers the conformal map,

$$\Phi(z) = z + i \cdot \Psi(z) \tag{1}$$

from G to an assembly of linear slits inclined at angles α_k. Here $\Psi(z)$ is analytic in G and $\Psi(\infty) = 0$, so Ψ can be represented as a sum of m Laurent series centered at the z_k's, (or, more precisely, the Taylor expansions centered at ∞ and converging in the exterior of the disks.) Given the circles and the normalization $z + O(1/z)$ at ∞ the map $\Phi(z)$ is uniquely determined by standard theorems; see [13, Thm 17.6a]. The example from [3] in Fig. 1 illustrates the map. Since $\Phi(z)$ can be continued analytically by reflection across the circles into the interior of the disks, as in, e.g., [9], the series converge geometrically.

We will use the notation in [3] for ease of comparison.

The m circles $C_k, k = 1, \ldots, m$ are parametrized by $z_{|k} := z_k + R_k e^{-it}, t \in [0, 2\pi]$ with the domain G to the left. In general, we denote values of functions on the kth circle by, e.g., $\Phi_{|k} := \Phi(z_{|k}) = z_{|k} + i\Psi_{|k}$. Since Φ maps the kth circle to a slit of inclination α_k, it must satisfy

$$\text{Im}\left[e^{-i\alpha_k} \cdot \Phi_{|k}\right] = A_k, \ \text{constant.}$$

Wegmann converts this into a boundary condition for $\Psi(z)$ as follows. Using $\Phi_{|k} = z_{|k} + i\Psi_{|k}$, we have that

$$
\begin{aligned}
\text{Im}\left[e^{-i\alpha_k} \cdot \Phi_{|k}\right] &= \text{Im}\left[e^{-i\alpha_k} \cdot \left(z_k + R_k e^{-it} + i \cdot \Psi_{|k}\right)\right] \\
&= \text{Im}\left[e^{-i\alpha_k} z_k\right] + R_k \text{Im}\left[e^{-i(\alpha_k + t)}\right] + \text{Im}\left[ie^{-i\alpha_k}\Psi_{|k}\right] \\
&= \text{Im}\left[e^{-i\alpha_k} z_k\right] - R_k \sin(t + \alpha_k) + \text{Re}\left[e^{-i\alpha_k}\Psi_{|k}\right] \\
&= A_k
\end{aligned}
$$

giving the boundary conditions,

$$\text{Re}\left[e^{-i\alpha_k} \cdot \Psi_{|k}(t) + a_{k0}\right] = R_k \sin(t + \alpha_k) =: \psi_k(t), \tag{2}$$

where $t \in [0, 2\pi], k = 1, \ldots, m$, and $a_{k0} := \text{Im}\left[e^{-i\alpha_k} z_k\right] - A_k$ are m real unknowns.

2.1. Riemann–Hilbert (R–H) problems

Wegmann [3] states the following theorem.

Theorem 1. *For any integer $l \geq 0$ and for any sufficiently smooth functions ψ_k on the boundary of G the R–H problem*

$$\text{Re}\left(e^{i\lambda_k} e^{ilt} \Psi_{|k} + a_{kl} e^{ilt} + \cdots + a_{k1} e^{it} + a_{k0}\right) = \psi_k,$$

has a unique solution consisting of an analytic function Ψ in G, with $\Psi(\infty) = 0$, and complex numbers $a_{k1}, \ldots, a_{kl}$ and real a_{k0}.

Here we just consider the case $l = 0$ and we have $\lambda_k = -\alpha_k$, the inclination angles of the slits. Additional theoretical discussion and applications can also be found in, e.g. [12], and references therein.

3. Solutions of Riemann–Hilbert problem

We will first represent $\Psi(z)$ from (1) in terms of a sum of Laurent series converging in the exterior of the m circles,

$$\Psi(z) = \sum_{k=1}^{m} h_k(z), \tag{3}$$

where

$$h_k(z) = \sum_{j=1}^{\infty} b_{j,k}(z - z_k)^{-j}, \tag{4}$$

and $b_{j,k}$ are the Laurent coefficients for the function $h_k(z)$. All of the methods here solve for the $b_{j,k}$'s. (The least squares method below includes weight factors R_k^j in the Laurent series.)

3.1. Wegmann's successive conjugation method

Observe that

$$\Psi_{|k} = \sum_{v=1}^{m} h_{v|k} = h_{k|k} + \sum_{v \neq k} h_{v|k}. \tag{5}$$

Wegmann [4,3] proposed a method of successive approximation based on (5). The iterations start with functions $h_k^{(0)}$. We may take all $h_k^{(0)} = 0$. The $h_k^{(n+1)}$'s are determined successively, for $k = 1, \ldots, m$, from the equations

$$\mathrm{Re}\left(e^{-i\alpha_k} h_{k|k}^{(n+1)} + a_{k0}\right) = \psi_k - \mathrm{Re}\left(e^{-i\alpha_k} \sum_{v < k} h_{v|k}^{(n+1)}\right) - \mathrm{Re}\left(e^{-i\alpha_k} \sum_{v > k} h_{v|k}^{(n)}\right)$$

$$=: \psi_k^*. \tag{6}$$

This is the Gauss–Seidel iteration. Wegmann [4] also considers a Jacobi iteration, but the method is somewhat slower. Next take FFT of the RHS of (6) to get the Fourier coefficients $A_{j,k}$ of ψ_k^*. Then

$$a_{k0} = A_{0,k},$$
$$b_{j,k} = 2R_k^j e^{-i\alpha_k} A_{j,k} \quad \text{for } j = 1, 2, \ldots. \tag{7}$$

The number of FFT points on each circle is N, for all m circles. $t \in [0, 2\pi)$ is discretized as $t_n = 2\pi(n-1)/N$ for $n = 1, \ldots, N$. The number of Laurent coefficients is $J = N/2$. The number of iterations for Wegmann's method to converge depends on the separation of the circles; see [4] for an analysis of convergence. (The case where $l, \alpha_k = 0$ is the modified Dirichlet problem. It is interesting to note that Wegmann's iteration above is essentially the Schwarz alternating method discussed in [14, Sec. 50] and applied to the case of circular boundaries; see also [15].) We give some segments of our MATLAB code in the Appendix.

3.2. Least squares (ls) method

Our new least squares approach introduces weights R_k^j in the expression for $h_k(z)$ and solves for both the $b_{j,k}$'s and the a_{k0}'s. Only the $b_{j,k}$'s are needed. The a_{k0}'s are discarded, as in Wegmann's method of successive conjugation. One can solve an overdetermined system for the $b_{j,k}$'s alone by subtracting the BCs at successive Fourier points to eliminate the constant a_{k0}'s on each circle as in [9], but this does not change the results very much, the singular values are less well-grouped, and the analysis is not as clear. We now use the Laurent series

$$h_k(z) = \sum_{j=1}^{\infty} b_{j,k} \cdot R_k^j \cdot (z - z_k)^{-j}. \tag{8}$$

The function $\Psi(z)$ defined in (3) then becomes

$$\Psi(z) = \sum_{k=1}^{m} h_k(z) = \sum_{k=1}^{m} \sum_{j=1}^{\infty} b_{j,k} \cdot R_k^j \cdot (z - z_k)^{-j}. \tag{9}$$

The boundary conditions for Φ in (2) for all $k = 1, \ldots, m$, are again

$$\text{Re}\left[e^{-i\alpha_k} \cdot \Psi_{|k}(t) + a_{k0}\right] = R_k \sin(t + \alpha_k). \tag{10}$$

From (9) we have

$$\Psi_{|k} = \sum_{v=1}^{m} h_{v|k} = \sum_{v=1}^{m} \sum_{j=1}^{\infty} b_{j,v} \cdot R_v^j \cdot (z_{|k} - z_v)^{-j}.$$

The boundary conditions in (10), with the Laurent series truncated at J terms become, for all $k = 1, \ldots, m$,

$$\text{Re}\left[e^{-i\alpha_v} \cdot \sum_{v=1}^{m} \sum_{j=1}^{J} b_{j,v} \cdot R_v^j \cdot (z_k + R_k e^{-it} - z_v)^{-j} + a_{k0}\right] = R_k \sin(t + \alpha_k). \tag{11}$$

We apply these at N Fourier points, $t = t_n = 2\pi(n-1)/N$, $n = 1, \ldots, N$ on each circle and solve the resulting least squares problem.

3.3. Matrix formulation

Using

$$h_{k|v}(t) = \sum_{j=1}^{J} b_{j,k} \cdot R_k^j \cdot (R_v e^{-it} + z_v - z_k)^{-j},$$

suppose t is discretized to N Fourier points on each circle. Then

$$h_{k|v}(t_n) = \sum_{j=1}^{J} b_{j,k} \cdot R_k^j \cdot (R_v e^{-it_n} + z_v - z_k)^{-j}. \tag{12}$$

Setting $z_{kv} = z_v - z_k$, define the $N \times J$ matrix,

$$H_{kv} = \begin{bmatrix} R_k^1(R_v e^{-it_1} + z_{kv})^{-1} & \cdots & R_k^J(R_v e^{-it_1} + z_{kv})^{-J} \\ \vdots & & \vdots \\ R_k^1(R_v e^{-it_N} + z_{kv})^{-1} & \cdots & R_k^J(R_v e^{-it_N} + z_{kv})^{-J} \end{bmatrix}, \tag{13}$$

and the $J \times 1$ vector,

$$b_k = \begin{bmatrix} b_{1,k}, & \cdots, & b_{J,k} \end{bmatrix}^T. \tag{14}$$

Then $h_{k|v}(t)$ in vector form becomes

$$h_{k|v} = H_{kv} b_k. \tag{15}$$

Next, define the $mN \times mJ$ matrix,

$$H = \begin{bmatrix} H_{11} & \cdots & H_{1m} \\ \vdots & & \vdots \\ H_{m1} & \cdots & H_{mm} \end{bmatrix}, \tag{16}$$

and the $mJ \times 1$ vector

$$b = \begin{bmatrix} b_1 \\ \vdots \\ b_m \end{bmatrix}. \tag{17}$$

Further, define a $mN \times m$ matrix P such that

$$P = \begin{bmatrix} 1_N & 0_N & \cdots & 0_N \\ 0_N & 1_N & \cdots & 0_N \\ \vdots & \vdots & & \vdots \\ 0_N & 0_N & \cdots & 1_N \end{bmatrix}, \tag{18}$$

where the N-vectors $1_N = [1, \ldots, 1]^T$ and $0_N = [0, \ldots, 0]^T$. In addition, to account for the orientation, α_k, of the slits, set

$$L_k = e^{-i\alpha_k} \cdot I_N \tag{19}$$

$$L = \begin{bmatrix} L_1 & Z_N & \cdots & Z_N & Z_N \\ \vdots & & & & \vdots \\ Z_N & \cdots & L_k & \cdots & Z_N \\ \vdots & & & & \vdots \\ Z_N & Z_N & \cdots & Z_N & L_m \end{bmatrix}, \tag{20}$$

where I_N is the $N \times N$ identity matrix and Z_N is the $N \times N$ matrix of zeros. Here (and in the MATLAB code), we also denote

$$A := LH, \quad \text{an } mN \times mJ \text{ complex matrix,}$$
$$ARI := [\text{Re}\,(LH) \quad -\text{Im}\,(LH)], \quad \text{an } mN \times mN \text{ real matrix,} \quad \text{and}$$
$$AS := [ARI\ P], \quad \text{an } mN \times (mN + m) \text{ real matrix.}$$

Also, let $a = [a_{10}, \ldots, a_{k0}, \ldots, a_{m0}]^T$ and define the vectors

$$b_a := \begin{bmatrix} \text{Re}\,b \\ \text{Im}\,b \\ \hline a \end{bmatrix},$$

$$\psi := \begin{bmatrix} \psi_1 \\ \vdots \\ \psi_m \end{bmatrix},$$

where $\psi_k = [\psi_k(t_1), \ldots, \psi_k(t_N)]^T$. We then solve the $mN \times (mN + m)$ system

$$AS b_a = \psi \tag{21}$$

by the MATLAB backslash or by conjugate gradient for the normal equations using `cgls` from [16].

3.4. Analysis of the matrices

We show here that $AS/\sqrt{N/2}$ has singular values well-grouped around one. Therefore, $AS^T AS$ has the form of the identity plus a low rank matrix and conjugate gradient for the normal equations will converge rapidly. To illustrate the properties of the matrices, we first analyze $A = LH$ for a simple case with $m = 2$ and $\alpha_k = 0$, $k = 1, 2$, so that $L = I$ and $A = H$. In block form,

$$H = \begin{bmatrix} H_{11} & H_{12} \\ H_{21} & H_{22} \end{bmatrix}.$$

A slit map with horizontal slits (nearly touching) is displayed in Fig. 2. Note that the diagonal blocks, $k = \nu$, $H_{kk} = [e^{i2\pi lj/N}]$, $l = 0, \ldots, N - 1$, $j = 1, \ldots, J = N/2$, are $N \times J$ matrices with the nice form of J columns of the DFT matrix,

$$H_{kk} = \begin{bmatrix} e^{it_1} & \cdots & e^{iJt_1} \\ \vdots & & \vdots \\ e^{it_N} & \cdots & e^{iJt_N} \end{bmatrix}. \tag{22}$$

We first find their singular values and then find the singular values of their real and imaginary parts. This will allow us to explain the singular values of ARI and finally AS.

Note that the Hermitian transpose is $H_{kk}^* = [e^{-i2\pi lj/N}]$. We now show that

$$\frac{1}{N} H_{kk}^* H_{kk} = I_{N/2},$$

the $N/2 \times N/2$ identity. The (l, j)th entry of $\frac{1}{N} H_{kk}^* H_{kk}$, $k = 1, 2$ is, e.g., for $k = 1$,

$$\frac{1}{N}(H_{11}^* H_{11})_{l,j} = \frac{1}{N} \sum_{k=0}^{N-1} e^{-i2\pi lk/N} e^{i2\pi kj/N}$$

$$= \frac{1}{N} \sum_{k=0}^{N-1} e^{i2\pi (j-l)k/N}$$
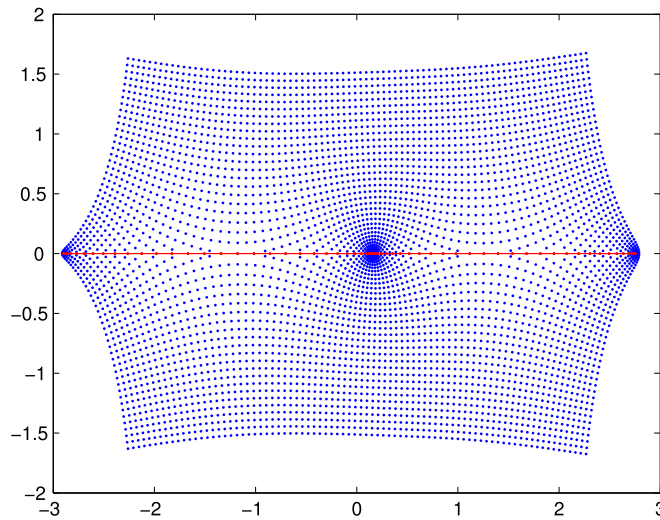
Fig. 2. Plot of map from exterior of $m = 2$ disks with $z_1 = -1$, $z_2 = 1$, $R_1 = 0.9$, $R_2 = 0.8$, $N = 32$. The slits are horizontal, so the inclination angles are $\alpha_1 = \alpha_2 = 0$. Since the circles nearly touch, the slits nearly touch. Images of $2N = 64$ Fourier points are plotted along the slits.

$$= \frac{1}{N} \begin{cases} N, & \text{if } l = j \ (e^{i2\pi(j-l)} = 1) \\ \dfrac{1 - e^{i2\pi(j-l)}}{1 - e^{i2\pi(j-l)/N}}, & \text{if } l \neq j \ (e^{i2\pi(j-l)} \neq 1) \end{cases}$$

$$= \begin{cases} 1, & \text{if } l = j \\ 0, & \text{if } l \neq j. \end{cases}$$

For the off-diagonal blocks $H_{k\nu}$, $k \neq \nu$, of H from (13) with the weights R_k^j, we see that the entries decrease like powers of $R_k / |R_\nu + z_{k\nu}| < 1$. As a result, the singular values of $H_{k\nu}$, $k \neq \nu$, decay to 0 as N increases. The singular values of the blocks of $H / \sqrt{N}$ are plotted in Fig. 3.

To analyze the other matrices, ARI, AS, in our calculations, we find the singular values of the real and imaginary parts of H_{kk}. We use, for $l, j = 1, \ldots, N/2$, the calculation,

$$\frac{1}{N} \sum_{k=0}^{N-1} \cos(2\pi(l+j)k/N) = \frac{1}{N} \text{Re} \left\{ \sum_{k=0}^{N-1} e^{i2\pi(l+j)k/N} \right\}$$

$$= \frac{1}{N} \text{Re} \begin{cases} \dfrac{1 - e^{i2\pi(j+l)}}{1 - e^{i2\pi(j+l)/N}}, & \text{if } l \neq N/2 \text{ or } j \neq N/2 \\ N, & \text{if } l = j = N/2 \end{cases}$$

$$= \begin{cases} 0, & \text{if } l \neq N/2 \text{ or } j \neq N/2 \\ 1, & \text{if } l = j = N/2. \end{cases}$$

For $H_{kk}^R := \text{Re } H_{kk} = [\cos(2\pi l j/N)]$, $j = 0, 1, \ldots, N-1$, $l = 1, \ldots, N/2$ this gives

$$\frac{2}{N} ((H_{11}^R)^T H_{11}^R)_{l,j} = \frac{2}{N} \sum_{k=0}^{N-1} \cos(2\pi lk/N) \cos(2\pi kj/N)$$

$$= \frac{1}{N} \sum_{k=0}^{N-1} \cos(2\pi(j-l)k/N) + \cos(2\pi(j+l)k/N)$$

$$= \frac{1}{2N} \text{Re} \left\{ \sum_{k=0}^{N-1} e^{i2\pi(j+l)k/N} + e^{i2\pi(j-l)k/N} \right\}$$

$$= \begin{cases} 2, & \text{if } l = j = N/2 \\ 1, & \text{if } l = j \neq N/2 \\ 0, & \text{if } l \neq j. \end{cases}$$

Therefore, the $J = N/2$ singular values of $\text{Re } H_{kk} / \sqrt{J} = \sqrt{2}, 1, \ldots, 1$.
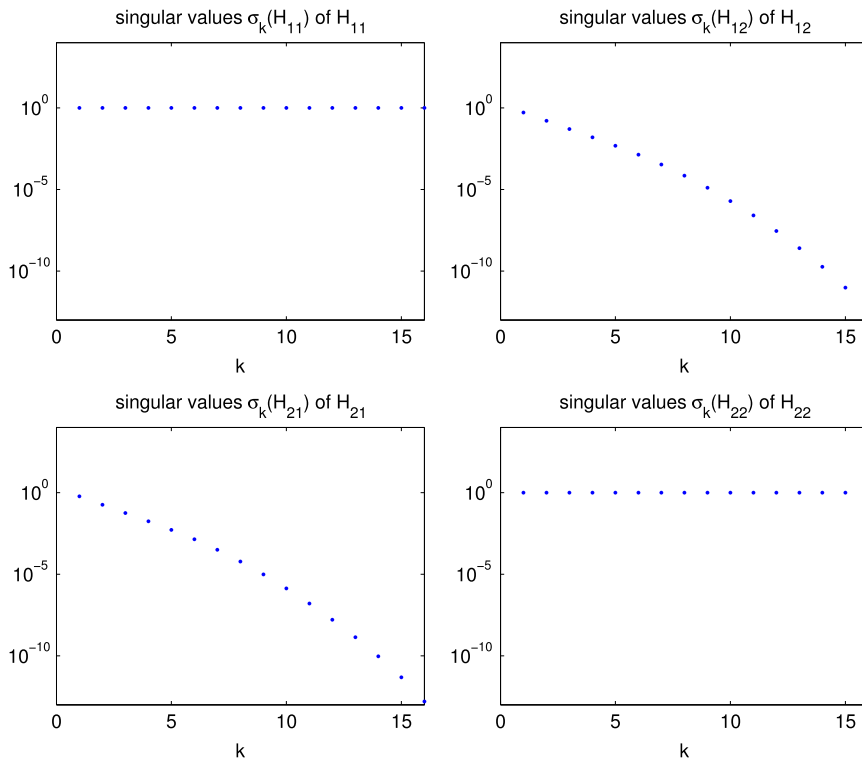
Fig. 3. Singular values of submatrices of $H/\sqrt{N}$ for $m = 2$, $z_1 = -1$, $z_2 = 1$, $R_1 = 0.9$, $R_2 = 0.8$, $\alpha_1 = \alpha_2 = 0$, $N = 32$.

Similarly, for $H_{kk}^I := \mathrm{Im}\, H_{kk} = [\sin(2\pi lj/N)]$, $l = 1, \ldots, N/2$, $j = 0, 1, \ldots, N - 1$, we have

$$\frac{2}{N}((H_{11}^I)^T H_{11}^I)_{l,j} = \frac{2}{N}\sum_{k=0}^{N-1} \sin(2\pi lk/N)\sin(2\pi kj/N)$$

$$= \frac{1}{N}\sum_{k=0}^{N-1} \cos(2\pi(j-l)k/N) - \cos(2\pi(j+l)k/N)$$

$$= \frac{1}{2N}\mathrm{Re}\left\{\sum_{k=0}^{N-1} e^{i2\pi(j+l)k/N} - e^{i2\pi(j-l)k/N}\right\}$$

$$= \begin{cases} 1, & \text{if } l = j \neq N/2 \\ 0, & \text{if } l = j = N/2 \\ 0, & \text{if } l \neq j. \end{cases}$$

Therefore, the $N/2$ singular values of $\mathrm{Im}\, H_{kk}/\sqrt{N/2} = 1, 1, \ldots, 1, 0$. The addition of the rows from the P matrix perturbs the eigenvalues according to standard theorems, e.g., [17, sec. 8.1.2], and the final matrix is nonsingular; see Fig. 5.

For small R_k, the off-diagonal matrix blocks have singular values that decay rapidly and perturb the singular values of the diagonal block matrix only slightly. The matrix *ARI* will therefore have roughly m singular values equal to $\sqrt{2}$ and m singular values equal to 0. Note the singular values of the $mN \times m$ matrix $P/\sqrt{J}$ are just m values of $\sqrt{2}$. Therefore, adding the m columns of P to *ARI* yields a full rank matrix *AS* with m $\sqrt{2}$'s replacing the m 0's of *ARI*. That is the $mN \times (mN + m)$ matrix $AS/\sqrt{J}$ has $2m$ singular values equal to $\sqrt{2}$ and $mN - 2m$ equal to 1 (slightly perturbed by the off-diagonal blocks). This is illustrated in Fig. 4 for $m = 2, 3$ and taking only $N = 8$ to clearly display the singular values. For larger R_k's these singular values are perturbed more.

3.5. Convergence of cgls

AS is of the form *constant · identity plus low rank*, so cgls converges superlinearly and is independent of N. This and the linear convergence of Wegmann's method are illustrated in Fig. 6. The number of cgls iterations is also proportional to the connectivity m and dependent on how close the circles are to touching; see Table 2. The number of singular values (square roots of eigenvalues) of $AS/\sqrt{J}$ which are not equal to 1 is the rank of the perturbation of the identity and therefore gives a
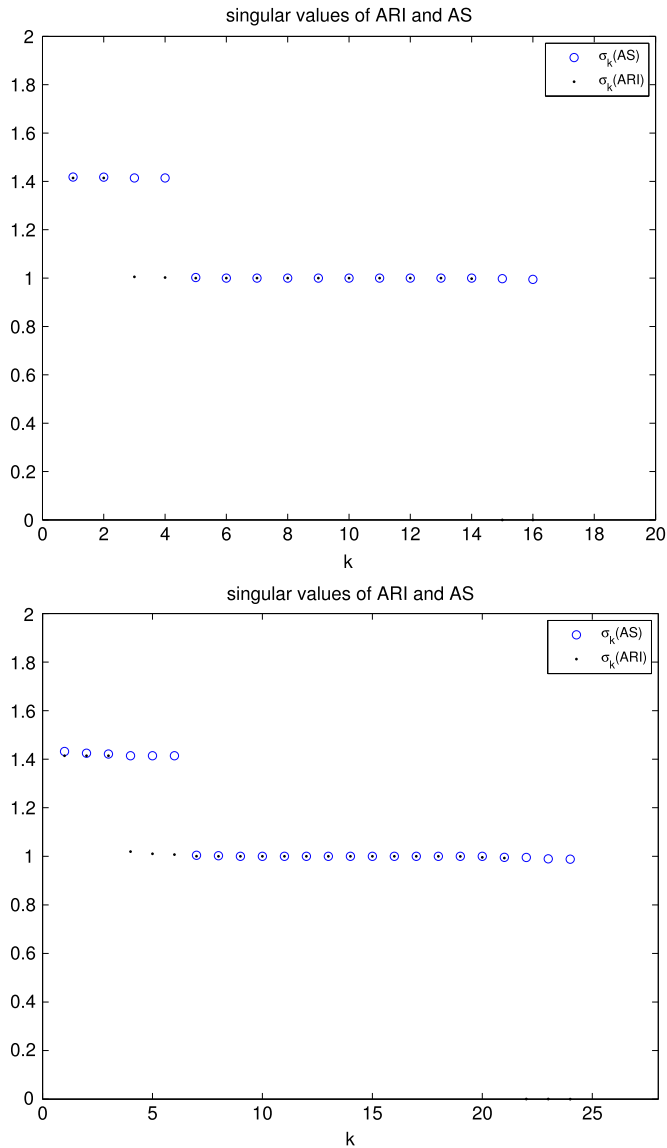
Fig. 4. Singular values of $ARI/\sqrt{J}$ and $AS/\sqrt{J}$ for $m = 2$, 3 disks with $z_1 = -1$, $z_2 = 1$, $z_3 = i$, $R_1 = R_2 = R_3 = 0.1$, $\alpha_1 = \alpha_2 = \alpha_3 = 0$, $N = 8$ illustrating $2m\sqrt{2}$ singular values (O) for $AS/\sqrt{J}$ and m 0 and $\sqrt{2}$ singular values ($\cdot$) for $ARI/\sqrt{J}$.

rough estimate of the number of `cgls` iterations according to standard theorems for the convergence of conjugate gradient methods; see [17, Sec. 10.2]. In general, however, we can expect the number of iterations for `cgls` to roughly increase linearly with the connectivity m and as the R_k's approach 1. More examples are given in the next section.

4. Numerical examples

We measure our *errors* by rotating the slits to the horizontal and taking the difference of the imaginary parts with the average value at $2N$ Fourier points, $t_n = \pi(n-1)/N$, $n = 1, \ldots, 2N$, on the boundary circles. Let

$$\varepsilon_{k,n} := \left| \text{Im}\left[e^{-i\alpha_k} \Phi_{|k}(t_n) \right] - \text{average}[\text{Im}(e^{-i\alpha_k} \Phi_{|k}(t_n))] \right|. \tag{23}$$

Then the overall error ε is

$$\varepsilon_k := \max_n \varepsilon_{k,n} \tag{24}$$

$$\varepsilon = \max_k \varepsilon_k. \tag{25}$$
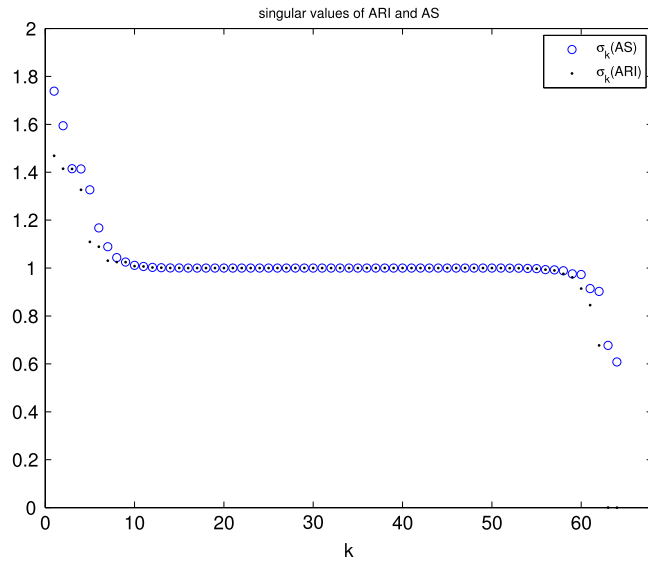
Fig. 5. Singular values of matrices $ARI/\sqrt{J}$ and $AS/\sqrt{J}$ for $m = 2, z_1 = -1, z_2 = 1, R_1 = 0.9, R_2 = 0.8, \alpha_1 = \alpha_2 = 0, N = 32$.
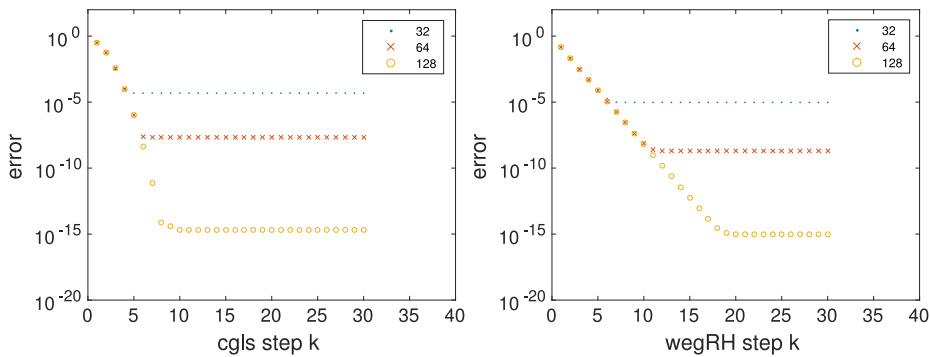
Fig. 6. The convergence of the errors ε for cgls (left) and Wegmann's Gauss–Seidel iteration (right) for $N = 32, 64, 128$ for two collinear slits $m = 2, \alpha_1 = \alpha_2 = 0, z_1 = -1, z_2 = 1, R_1 = R_2 = 0.9$ are plotted. The linear convergence of Wegmann's method and the superlinear convergence of cgls are evident, along with the independence of the rates from N until the level of discretization error is reached.

ε gives a measure of how straight the computed slits are and how close they are to having the correct inclinations, α_k. Also, the coefficients, $b_{k,j}$, computed by the three methods for various N agree to about the same level of accuracy as the errors, ε, so we have not reported them below.

Example 1. The three methods are first compared on a domain with $m = 5$, Fig. 7. The errors and timings in Table 1 indicate that the methods are roughly comparable with cgls somewhat less accurate. Note the approximate spectral accuracy of the error (when N is doubled the error approximately squares). The level of accuracy is least on the large circle. The operation counts are $O((mN)^3)$ for *ls*, the MATLAB backslash, and $O(k_\epsilon (mN)^2)$ for cgls and Wegmann's Gauss–Seidel iterations, where k_ϵ is the number of iterations needed to reach the level of discretization error. (We have not implemented a stopping rule based on our error estimate.) The timings roughly fit the operations count with the *ls* method slightly slower than the iterative methods.

Remark. Changing the α_k's has little effect on the behavior of the methods, since the errors depend mainly on the relative size and nearness of the circles. The convergence seems to depend only on the separation of the circles, due to the reflection argument above, in Section 2. The symmetry or the inclination of the slits does not affect convergence, since the circles are given as input. However, for the same circles collinear or oblique slits will be much closer to touching than parallel slits. This is consistent with the examples in [7] where the slit-like domains are specified first and the centers and radii of the circles have to be computed along with the Laurent series—a more difficult problem. There are practical limits to what one can expect to compute effectively in cases where the slits and circles are close. We plan to investigate such cases more fully in the future.
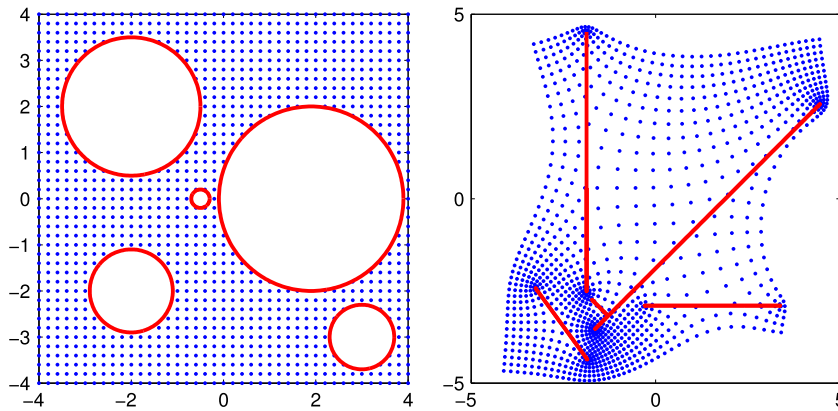
Fig. 7. Map for example with $m = 5$.

Table 1

Comparison of typical timings in seconds on a laptop running MATLAB version R2012a, for $m = 5$ example, radius $=$ [2 0.2 0.7 1.5 0.9], center $=$ [1.9 -0.5 3 $-$ 3i $-$ 2 $+$ 2i $-$ 2 $-$ 2i], alpha $=$ [0.25 $*$ pi $-$ 0.25 $*$ pi 0 0.5 $*$ pi $-$ 0.3 $*$ pi]. We stop the cgls and wegrhGS iterations a few iterations after the error stops decreasing.

N	ls (s)	Error	cgls(k_ϵ)	Error	wegrhGS(k_ϵ)	Error
32	0.008	$4.5 \cdot 10^{-3}$	0.007(15)	$1.0 \cdot 10^{-1}$	0.009(10)	$3.9 \cdot 10^{-3}$
64	0.03	$2.6 \cdot 10^{-4}$	0.02(20)	$1.2 \cdot 10^{-3}$	0.02(10)	$2.2 \cdot 10^{-4}$
128	0.13	$7.9 \cdot 10^{-7}$	0.07(20)	$4.9 \cdot 10^{-5}$	0.07(10)	$6.8 \cdot 10^{-7}$
256	1.07	$1.0 \cdot 10^{-11}$	0.35(30)	$3.2 \cdot 10^{-9}$	0.29(15)	$9.5 \cdot 10^{-12}$
512	6.84	$6.4 \cdot 10^{-14}$	1.20(35)	$5.8 \cdot 10^{-14}$	1.06(20)	$5.7 \cdot 10^{-14}$

Table 2

Comparison of typical timings in seconds on a laptop running MATLAB version R2012a, α's $= 0$, centers $= \pm 2 \pm 2i$, ... for various m, N, and R_j's. Solutions are given for up to 4096 unknowns, Re $b_{j,k}$, Im $b_{j,k}$.

m	R_j	N	ls (s)	Error	cgls(k_ϵ)	Error	wegrhGS(k_ϵ)	Error
8		16	0.01	$3.2 \cdot 10^{-6}$	0.01(15)	$2.7 \cdot 10^{-5}$	0.01(7)	$3.3 \cdot 10^{-6}$
		32	0.02	$4.8 \cdot 10^{-11}$	0.02(25)	$6.7 \cdot 10^{-10}$	0.02(10)	$4.9 \cdot 10^{-11}$
	0.5	64	0.06	$6.0 \cdot 10^{-15}$	0.21(30)	$1.0 \cdot 10^{-14}$	0.06(15)	$4.2 \cdot 10^{-15}$
16		16	0.02	$3.2 \cdot 10^{-6}$	0.01(12)	$3.2 \cdot 10^{-5}$	0.04(10)	$3.2 \cdot 10^{-6}$
		32	0.07	$4.8 \cdot 10^{-11}$	0.04(20)	$8.2 \cdot 10^{-10}$	0.08(15)	$4.8 \cdot 10^{-11}$
		64	0.61	$1.2 \cdot 10^{-14}$	0.18(25)	$6.7 \cdot 10^{-15}$	0.24(20)	$5.8 \cdot 10^{-15}$
8	0.9	32	0.02	$6.9 \cdot 10^{-5}$	0.01(35)	$1.7 \cdot 10^{-4}$	0.02(15)	$6.9 \cdot 10^{-5}$
		64	0.07	$1.9 \cdot 10^{-8}$	0.05(50)	$1.0 \cdot 10^{-7}$	0.07(25)	$2.0 \cdot 10^{-8}$
		128	0.55	$3.3 \cdot 10^{-14}$	0.28(70)	$2.0 \cdot 10^{-14}$	0.35(50)	$7.7 \cdot 10^{-15}$
16	0.9	32	0.07	$6.3 \cdot 10^{-5}$	0.04(25)	$2.5 \cdot 10^{-4}$	0.10(20)	$6.3 \cdot 10^{-5}$
		64	0.57	$1.8 \cdot 10^{-8}$	0.22(40)	$1.1 \cdot 10^{-7}$	0.30(30)	$1.8 \cdot 10^{-8}$
		128	3.81	$5.2 \cdot 10^{-14}$	0.89(70)	$1.0 \cdot 10^{-14}$	1.41(60)	$9.9 \cdot 10^{-15}$
8	0.99	32	0.02	$2.4 \cdot 10^{-2}$	0.01(30)	$3.3 \cdot 10^{-2}$	0.02(10)	$2.8 \cdot 10^{-2}$
		64	0.08	$1.6 \cdot 10^{-3}$	0.06(80)	$1.6 \cdot 10^{-3}$	0.09(40)	$1.6 \cdot 10^{-3}$
		128	0.60	$9.9 \cdot 10^{-6}$	0.41(120)	$1.4 \cdot 10^{-5}$	0.55(80)	$1.0 \cdot 10^{-5}$
		256	3.72	$6.0 \cdot 10^{-10}$	1.65(160)	$7.7 \cdot 10^{-10}$	2.02(140)	$7.4 \cdot 10^{-10}$
		512	25.69	$1.0 \cdot 10^{-13}$	7.92(200)	$3.4 \cdot 10^{-14}$	12.45(220)	$1.7 \cdot 10^{-14}$
16	0.99	64	0.59	$1.4 \cdot 10^{-3}$	0.21(40)	$2.3 \cdot 10^{-3}$	0.37(40)	$1.6 \cdot 10^{-3}$
		128	3.63	$8.7 \cdot 10^{-6}$	1.15(80)	$1.3 \cdot 10^{-4}$	2.40(100)	$8.8 \cdot 10^{-6}$
		256	26.36	$5.3 \cdot 10^{-10}$	6.19(150)	$5.4 \cdot 10^{-10}$	9.64(170)	$5.3 \cdot 10^{-10}$

Example 2. Here we illustrate the effect of increasing the connectivity m and the radii of the circles for several cases in Table 2. Figs. 8–11 illustrate the maps, the singular values of $AS/\sqrt{J}$, and `cgls` convergence for two examples for Table 2. Again the behavior of the three methods is somewhat comparable with the iterative methods somewhat faster for larger mN and circles closer to touching. As the circles get close to touching, the eigenvalues of the matrix AS smear out and more conjugate gradient iterations are needed.
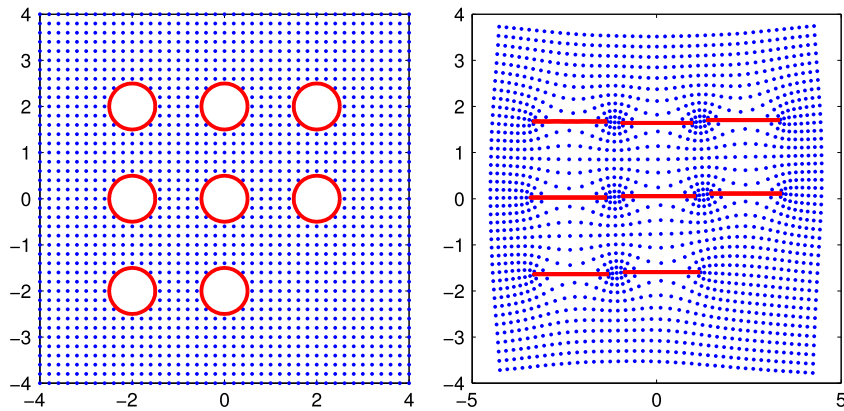
Fig. 8. Map for example with $m = 8$, $R_k = 0.5$, $N = 16$, $\alpha_k = 0$.
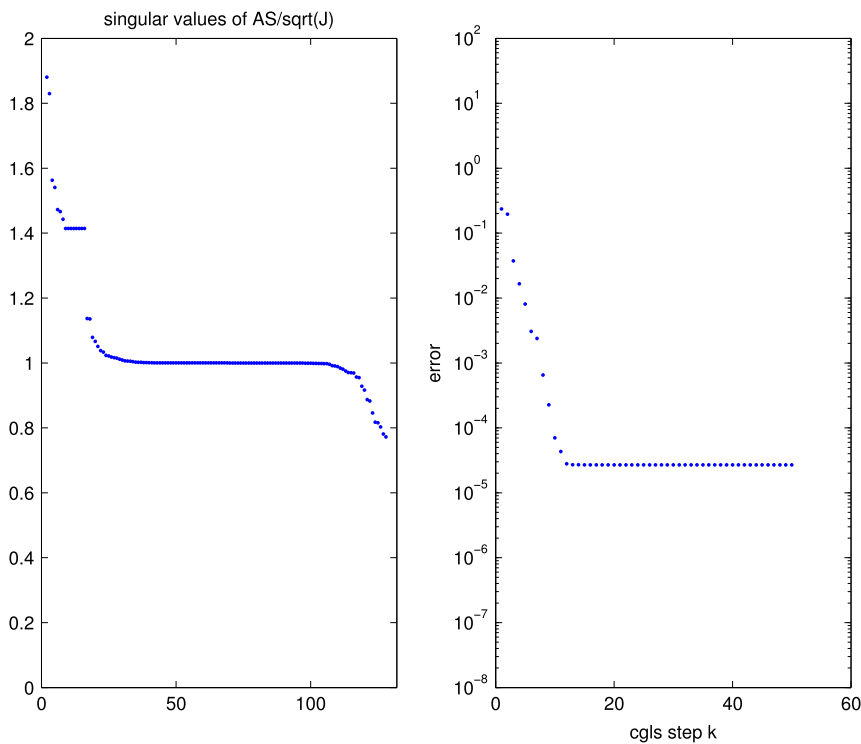
Fig. 9. Singular values of AS and errors ε in cgls iterations for example with $m = 8$, $R_k = 0.5$, $N = 16$, $\alpha_k = 0$.

4.1. Some variations

Other formulations are possible. In [9,6] the least squares approach is used with the MATLAB backslash without including the weight factors of R_k^j in the basis functions. This approach often leads to very ill-conditioned systems and inaccuracies. For instance, if R_2 is increased from 1.5 to 2.0 in Wegmann's example, the method fails for $N = 32$. The method can sometimes be made to work by adjusting N and J independently, but this is inconvenient. Also, as in [9], the need for solving for the a_{k0} can be avoided by subtracting successive boundary conditions at t_j's on each circle leading to a rectangular system for the $b_{k,j}$'s only and taking, say, $J = N/2 - 1$. However, this changes the results very little and the formulation is more ad hoc and the singular values are not well-grouped. Also note that [9] used $N = 300$, $J = 20$ on a similar problem to get a highly overdetermined system. This seems unnecessary here and more difficult to analyze.

Adding R_k^j's to the Wegmann successive conjugation makes no difference, presumably because these factors are already included in the calculation of the $b_{k,j}$'s.
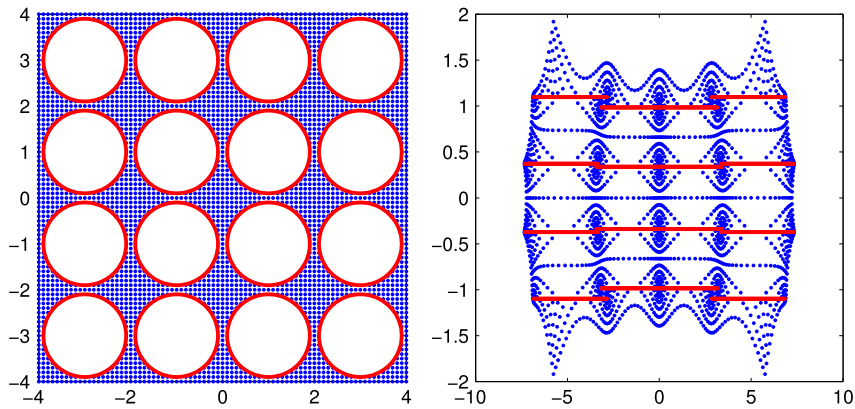
Fig. 10. Map for example with $m = 16$, $R_k = 0.9$, $N = 64$, $\alpha_k = 0$.
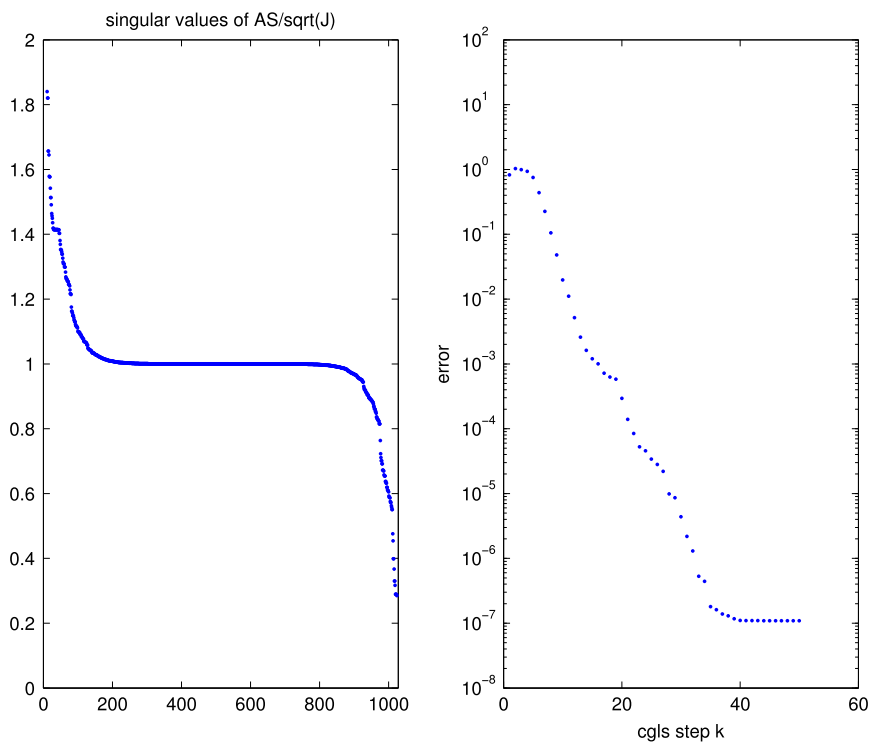
Fig. 11. Singular values of *AS* and errors ε in cgls iterations for example with $m = 16$, $R_k = 0.9$, $N = 64$, $\alpha_k = 0$.

5. Comments

We have compared various numerical approaches to solving a simple linear Riemann–Hilbert problem for multiply connected conformal maps from circular domains to slit domains and analyzed their behavior. There are related R–H problems, such as those in [8–11,4], which we plan to consider in the future and the analysis of this simple problem will be a useful guide for studying the related problems. The case where $l = 1$ occurs often in conformal mapping [10,11,1,2] and our least squares formulation should be applicable in this case.

Acknowledgments

Appendix. MATLAB **code**

```
% driver code for our slit map examples using backslash, cgls, and
% Wegmann's method method of successive conjugation method for RH
% problems using a Gauss--Seidel (GS) iteration; see Wegmann 2005,
% Wegmann's example, p. 461:
radius=[1 1.5 0.7]; center=[2 -1-2i -1+2i]; alpha = [0 pi/4 pi/2];
N=128; J=N/2; m=3; itmax=30;
z=zeros(N,m); t=2*pi*(0:N-1)'/N;
tic  % begin timing of common portions of code
for k=1:m
 z(:,k)=center(k)+radius(k)*exp(-1i*t); % N pts on circles clockwise
end
z=z(:);
  rhs=[];
for k=1:m
  rhs=[rhs; radius(k)*sin(t+alpha(k))];  % compute right hand side
end
onesR=radius;
%onesR=ones(1,m); % set radii to one in basisfunctions for Wegmann
A = basisfunctions(z,center, onesR, alpha, N, J, m);
%ARI = [real(A), -imag(A)]; % comment in to solve with \ or cgls
%z1=ones(N,1);                %                ''
%P=kron(eye(m),z1);          %                ''
% AS=[ARI,P];                 %                ''
%b=AS\rhs;                    %  solve with backslash
% itmax=20; number of cgls or Wegmann iterations
%%[B,rho,eta] = cgls(AS,rhs,itmax); %% comment in to solve with cgls
%%%[B,errb] = wegrh_GS(A,rhs,radius,alpha,itmax,N); %%% Wegmann GS
time=toc   % end timing
% plotting of output, svd's, errors,...,follow here...

function A = basisfunctions(z, center, radius, alpha, N, J, m)
%  Note: factors of radius(k)^j added to basisfunctions from [3]
%  input radius = ones(1,m) for Wegmann's methods
    for k = 1:m
      for j=1:J
        A(:,J*(k-1)+j) = (radius(k)./(z-center(k))).^j;
      end
    end
    for k=1:m
      ak = exp(-1i*alpha(k));  % mult. by exp of angles alpha(k)
      A(1+(k-1)*N:k*N,:)=ak*A(1+(k-1)*N:k*N,:);
    end
end

function [B,errb] = wegrh_GS(A,rhs,radius,alpha,itmax,N)
% Wegmann's R-H iteration from 2005 survey paper p. 459
% efficient Gauss--Seidel iteration with matrix mult
% psi = rhs, psi* = psis
m=length(alpha); J=N/2; z=zeros(N,m); psi=zeros(N,m);
b=zeros(J,m); bjac=b; B=zeros(m*J,itmax); berr=b; psis=psi;
t=2*pi*(0:N-1)'/N; ealpha=exp(1i*alpha);
  BGS = B(:,1);
for iter=1:itmax
   for ks=1:m
   psis(:,ks)=rhs(1+(ks-1)*N:ks*N);
   for k=1:ks-1
    psis(:,ks)=psis(:,ks)...
        - real(A(1+(ks-1)*N:ks*N,1+(k-1)*J:k*J)*BGS(1+(k-1)*J:k*J));
   end
```

```
  for k=ks+1:m
   psis(:,ks)=psis(:,ks)...
        - real(A(1+(ks-1)*N:ks*N,1+(k-1)*J:k*J)*BGS(1+(k-1)*J:k*J));
   end
   Aj=fft(psis(:,ks))/N;
   b(:,ks)=(2*ealpha(ks))*(radius(ks).^[1:J]').*(Aj(2:J+1));
   B(1+(ks-1)*J:ks*J,iter)=b(:,ks);
   errb(iter,ks)=norm(berr(:,ks)-b(:,ks));
   berr(:,ks)=b(:,ks);
   BGS(1+(ks-1)*J:ks*J)=b(:,ks);
  end
end
```

References

[1] V. Mityushev, Schwarz–Christoffel formula for multiply connected domains, Comput. Methods Funct. Theory 12 (2012) 449–463.
[2] R. Wegmann, Fast conformal mapping of multiply connected regions, J. Comput. Appl. Math. 130 (2001) 119–138.
[3] R. Wegmann, Methods for Numerical Conformal Mapping, in: R. Kuehnau (Ed.), Handbook of Complex Analysis, Geometric Function Theory, Vol. 2, Elsevier, 2005, pp. 351–477.
[4] R. Wegmann, Constructive solution of a certain class of Riemann–Hilbert problems on multiply connected circular domains, J. Comput. Appl. Math. 130 (2001) 139–161.
[5] M.D. Finn, S.M. Cox, H.M. Byrne, Topological chaos in inviscid and viscous mixers, J. Fluid Mech. 493 (2003) 345–361.
[6] L.N. Trefethen, Ten digit algorithms, Report No. 05/13, Oxford University Computing Laboratory, 2005.
[7] N. Benchama, T. DeLillo, T. Hrycak, L. Wang, A simplified Fornberg-like method for the conformal mapping of multiply connected regions—comparisons and crowding, J. Comput. Appl. Math. 209 (2007) 1–21.
[8] R. Czapla, V. Mityushev, N. Rylko, Conformal mapping of circular multiply connected domains onto slit domains, Electron. Trans. Numer. Anal. 39 (2012) 286–297.
[9] T.K. DeLillo, T.A. Driscoll, A.R. Elcrat, J.A. Pfaltzgraff, Radial and circular slit maps of unbounded multiply connected circle domains, Proc. R. Soc. Lond. Ser. A Math. Phys. Eng. Sci. 464 (2008) 1719–1737.
[10] T.K. DeLillo, A.R. Elcrat, E.H. Kropf, J.A. Pfaltzgraff, Efficient calculation of Schwarz–Christoffel transformations for multiply connected domains using Laurent series, Comput. Methods Funct. Theory 13 (2013) 307–336.
[11] T.K. DeLillo, E.H. Kropf, Slit maps and Schwarz–Christoffel maps for multiply connected domains, Electron. Trans. Numer. Anal. 36 (2010) 195–223.
[12] V. Mityushev, S. Rogosin, Constructive Methods for Linear and Nonlinear Boundary Value Problems for Analytic Functions: Theory and Applications, Chapman & Hall, 2000.
[13] P. Henrici, Applied and Computational Complex Analysis, Vol. 3, John Wiley, 1986.
[14] S.G. Mikhlin, Integral Equations and their Applications to Certain Problems in Mechanics, Mathematical Physics and Technology, Pergamon Press, 1964, Second revised edition.
[15] B. Bojarski, V. Mityushev, R-linear problem for multiply connected domains and alternating method of Schwartz, J. Math. Sci. 189 (1) (2013) 68–77.
[16] P.-C. Hansen, Regularization Tools: A Matlab Package for Analysis and Solution of Discrete Ill-Posed Problems, version 2.0 for Matlab 4.0 (1992, revised 1998); see Numer. Algor. 6 (1994) 1–35; software available via netlib@research.att.com from directory NUMERALGO.
[17] G.H. Golub, C.F. van Loan, Matrix Computations, Third ed., Johns Hopkins, 1996.